Junctional tumor suppressors interact with 14-3-3 proteins to control planar spindle alignment

Yu-ichiro Nakajima[1,2,3], Zachary T. Lee[1], Sean A. McKinney[1], Selene K. Swanson[1], Laurence Florens[1], and Matthew C. Gibson[1,4]

Proper orientation of the mitotic spindle is essential for cell fate determination, tissue morphogenesis, and homeostasis. During epithelial proliferation, planar spindle alignment ensures the maintenance of polarized tissue architecture, and aberrant spindle orientation can disrupt epithelial integrity. Nevertheless, in vivo mechanisms that restrict the mitotic spindle to the plane of the epithelium remain poorly understood. Here we show that the junction-localized tumor suppressors Scribbled (Scrib) and Discs large (Dlg) control planar spindle orientation via Mud and 14-3-3 proteins in the *Drosophila* wing disc epithelium. During mitosis, Scrib is required for the junctional localization of Dlg, and both affect mitotic spindle movements. Using coimmunoprecipitation and mass spectrometry, we identify 14-3-3 proteins as Dlg-interacting partners and further report that loss of 14-3-3s causes both abnormal spindle orientation and disruption of epithelial architecture as a consequence of basal cell delamination and apoptosis. Combined, these biochemical and genetic analyses indicate that 14-3-3s function together with Scrib, Dlg, and Mud during planar cell division.

Introduction

The orientation of the mitotic spindle is a critical determinant of the axis of cell division, and thus underlies the generation of cellular diversity and maintenance of tissue organization by coordinating division orientation with respect to polarized cues (Gillies and Cabernard, 2011; Morin and Bellaïche, 2011). In polarized epithelia, symmetric cell division predominates, such that the mitotic spindle aligns within the plane of the epithelium. This particular orientation of cell division, referred to as planar division, gives rise to two identical daughter cells and allows their tight integration in the epithelial monolayer. It follows that planar alignment of the mitotic spindle ensures the maintenance of epithelial architecture and preserves barrier function (Macara et al., 2014; Ragkousi and Gibson, 2014; Nakajima, 2018). Defects in planar division can disrupt tissue organization and may therefore lead to epithelial pathogenesis, epithelial-to-mesenchymal transition, and tumorigenesis (Pease and Tirnauer, 2011; Noatynska et al., 2012; Nakajima et al., 2013).

Mitotic spindle orientation relies on the polarized localization of force generators that link astral microtubules and the cell cortex. The conserved Partner of Inscuteable (Pins) complex (Gαi/Pins/Mud in *Drosophila melanogaster* and Gαi/LGN/NuMA in vertebrates) represents the core molecular machinery that controls mitotic spindle orientation during both asymmetric and symmetric cell division (Gillies and Cabernard, 2011; Morin and

Bellaïche, 2011; Lu and Johnston, 2013; di Pietro et al., 2016). During planar division in the vertebrate neuroepithelium and in mammalian epithelial culture, Pins/LGN localizes to the lateral cortex, where it binds to the membrane-anchored protein Gαi and allows for the positioning of the mitotic spindle via interaction with the microtubule-binding protein Mud/NuMA (Morin et al., 2007; Konno et al., 2008; Zheng et al., 2010; Peyre et al., 2011). In addition to this core machinery, in vitro studies have implicated adhesion molecules (e.g., E-cadherin, JAM-A) and polarity determinants (e.g., aPKC, Cdc42, Par-3) in the robust control of planar spindle orientation (Jaffe et al., 2008; Hao et al., 2010; Qin et al., 2010; Rodriguez-Fraticelli et al., 2010; Durgan et al., 2011; Tuncay et al., 2015; Gloerich et al., 2017). However, the in vivo mechanisms that spatially restrict spindle position to the plane of the epithelium remain poorly understood.

The polarity protein Discs large (Dlg), known as a neoplastic tumor suppressor in *Drosophila*, appears to have evolved as a key regulator of cell polarity and mitotic spindle orientation in multicellularity (Anderson et al., 2016). During development, Dlg and another neoplastic tumor suppressor, Scribbled (Scrib), accumulate at septate junctions and are required to establish epithelial polarity (Bilder and Perrimon, 2000). The loss of *scrib* or *dlg* in larval imaginal discs leads to a dramatic neoplastic

[1]Stowers Institute for Medical Research, Kansas City, MO; [2]Frontier Research Institute for Interdisciplinary Sciences, Tohoku University, Sendai, Japan; [3]Graduate School of Life Sciences, Tohoku University, Sendai, Japan; [4]Department of Anatomy and Cell Biology, University of Kansas School of Medicine, Kansas City, KS.

Correspondence to Yu-ichiro Nakajima: yuichiro.nakajima.d2@tohoku.ac.jp.

phenotype characterized by massive disc overgrowth and the loss of epithelial organization (Woods and Bryant, 1989; Bilder et al., 2000). In addition, Dlg contributes to the control of mitotic spindle orientation during asymmetric cell division in sensory organ precursors and neuroblasts (Bellaïche et al., 2001; Siegrist and Doe, 2005; Johnston et al., 2009). Recent reports indicate that Dlg regulates planar spindle orientation in the wing disc epithelium and the follicular epithelium (Bergstralh et al., 2013; Nakajima et al., 2013). In the latter, Dlg directs the localization of Pins to the lateral cortex during cell division, a mechanism conserved in the chick neuroepithelium (Bergstralh et al., 2013; Saadaoui et al., 2014). By contrast, in the wing disc epithelium, although Scrib is necessary (Nakajima et al., 2013), Pins appears to be dispensable for planar spindle orientation (Bergstralh et al., 2016), suggesting that a Pins-independent pathway may control planar spindle alignment. The precise molecular mechanism by which junction-associated Scrib and Dlg regulate the mitotic spindle in epithelia remains unclear, and it is unknown whether or not these proteins affect spindle dynamics during planar division.

Here we investigate the cellular and molecular mechanisms by which junctional tumor suppressors direct planar spindle alignment in the *Drosophila* wing disc epithelium. Live imaging analyses of mitotic cells reveal biphasic spindle movements during planar division and demonstrate that depletion of Scrib, Dlg, or Mud causes defective spindle rotation and abnormal planar orientation. Molecularly, we show that the PSD-95, Dlg, ZO-1 homology (PDZ) domains of Scrib are essential for the localization of Dlg at septate junctions in the apical mitotic zone, which is in turn required for proper spindle orientation. We further identify 14-3-3 proteins as novel interacting partners of Dlg and demonstrate their requirement in planar spindle orientation and, accordingly, in the maintenance of tissue architecture. These results suggest a new molecular pathway comprising the junction proteins Scrib and Dlg associated with Mud and 14-3-3, which collectively control planar spindle alignment in *Drosophila* imaginal disc epithelia.

Results

Dynamics of mitotic spindle movement during planar orientation in wing disc epithelial cells

The *Drosophila* wing imaginal disc is a pseudostratified epithelial monolayer composed primarily of elongated columnar cells. During larval stages, wing disc cells exhibit continuous cell proliferation. At the cellular level, upon initiation of mitosis, apical mitotic rounding accompanies a process of interkinetic nuclear migration (Meyer et al., 2011). The subsequent stages of cell division take place within a septate junction–delimited mitotic zone near the apical epithelial surface (Meyer et al., 2011; Nakajima et al., 2013). Although planar spindle orientation requires interactions between the mitotic apparatus and spatial cues, precisely how these molecular components affect the kinetics of spindle orientation is not well understood.

To determine the dynamics of mitotic spindle movement, we first performed time-lapse imaging of cell division in ex vivo–cultured wing imaginal discs. We used a centrosome-localized

GFP fusion protein (Centrosomin; Cnn-GFP) and a nuclear marker (His2Av-mRFP) to visualize the mitotic spindle poles and chromatin, respectively (Fig. 1, A and B; and Videos 1 and 2). By tracking the 3D coordinates of Cnn-GFP–positive spindle poles with a semiautomated procedure, we analyzed spindle pole movements relative to the apico-basal axis (θ; Fig. 1 C) and to the plane of the epithelium (ϕ; Fig. S1 A), allowing us to plot spindle orientation kinetics during cell division (Fig. 1 D and Fig. S1, B and C). Because Cnn-GFP localization matured during mitosis as mitotic nuclei moved to the apical region, our analysis concentrated on dividing cells at the surface of the epithelium from prometaphase until the onset of anaphase.

Our analysis of mitotic spindle movements revealed two types of planar spindle alignment, depending on the initial spindle configuration. Dividing cells of type 1 exhibited planar orientation of the mitotic spindle from the outset of prometaphase ($\theta < \pm30°$) and maintained planar orientation until the onset of anaphase despite minor fluctuations in θ (type 1, $n = 19/45$; Fig. 1, A and D; and Video 1). By contrast, in type 2 divisions, θ was initially out of the range of planar orientation ($\theta > \pm30°$), and mitotic spindles progressively reoriented and aligned toward planar orientation during subsequent time points (type 2, $n = 26/45$; Fig. 1, B and D; and Video 2). Then, once spindle alignment became planar, θ remained consistent until anaphase onset (Figs. 1 D and S1 C). Notably, in both division types, the relative z rotation speed changed between the first and second halves of the orientation process (Figs. 1 E and S1 D), suggesting that mitotic spindle movements gradually converged on planar orientation. Unlike these stereotypic spindle movements along the apico-basal axis, spindle movement within the epithelial plane exhibited random distribution, and ϕ varied drastically across dividing cells (Fig. S1 B).

Together, these results suggest that planar spindle orientation in wing disc epithelial cells occurs in two phases during prometaphase and metaphase: during the first phase, both type 1 and type 2 mitotic spindles quickly orient parallel to the epithelial plane (Figs. 1 E and S1 D). During the second phase, spindle movements are less pronounced, and planar orientation is maintained. Similar biphasic spindle movements are also observed during planar division in the chick neuroepithelium (Peyre et al., 2011), suggesting that mitotic spindle movements in columnar epithelial cells may be conserved throughout evolution. Our analyses also reveal that mitotic spindle orientation can change before metaphase, even for cells initially located out of the range of planar orientation. For our remaining studies of spindle regulation, we therefore analyzed spindle orientation during late mitotic phases (anaphase-telophase).

Randomized spindle movements in Mud-, Scrib-, and Dlg-depleted cells

Previously reported evidence indicates that the neoplastic tumor suppressors Scrib and Dlg, as well as the spindle pole–associated factor Mud, control planar spindle alignment in the wing disc epithelium (Nakajima et al., 2013). To understand how mitotic spindle movements are controlled by these molecules, we performed live imaging analyses of cell division in wing discs where *mud*, *scrib*, or *dlg* were depleted by RNAi
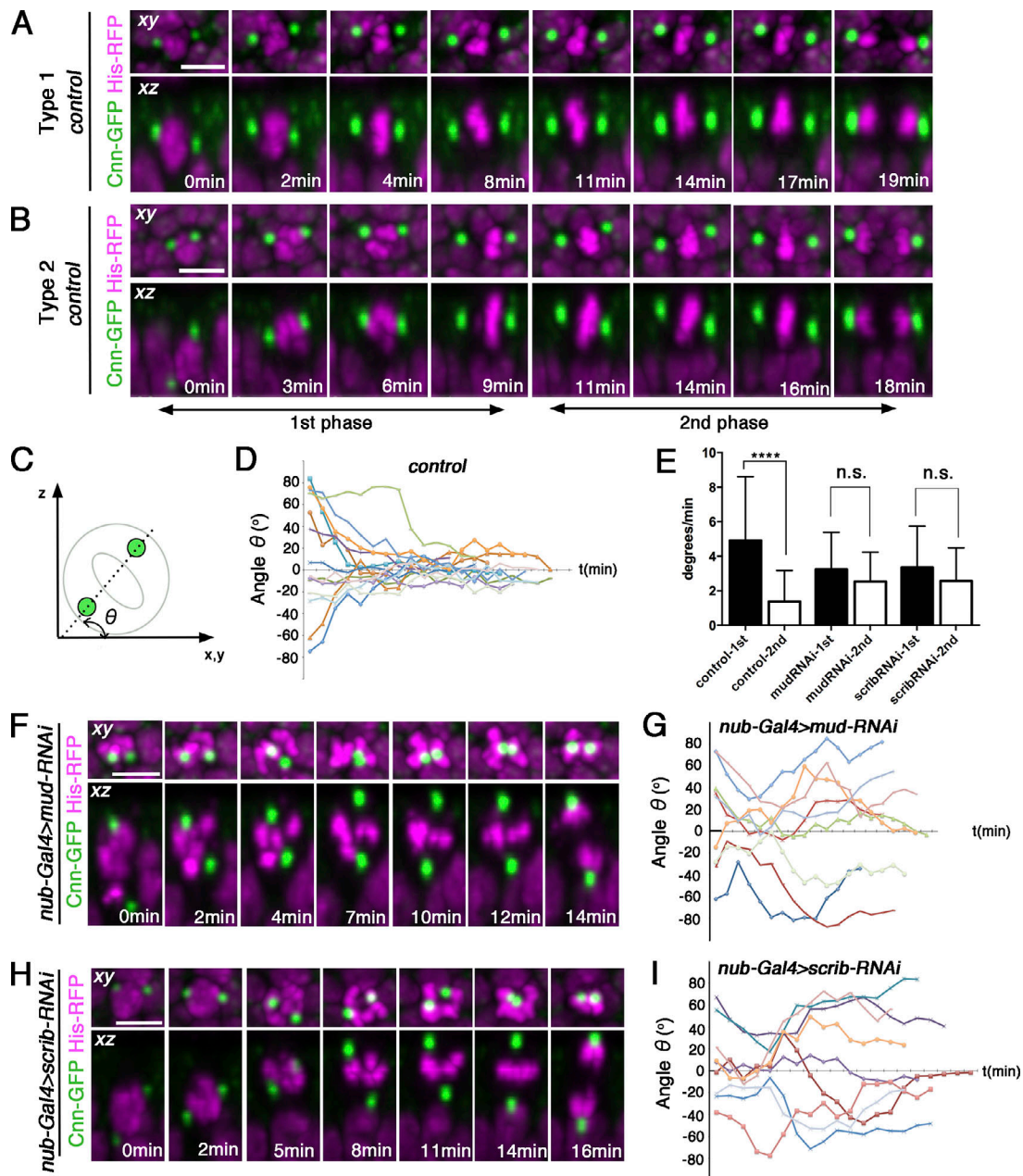
Nakajima et al.
Scrib/Dlg/14-3-3 control planar spindle alignment

Journal of Cell Biology 1825
https://doi.org/10.1083/jcb.201803116

Figure 1. **Mitotic spindle movements are randomized in Mud- and Scrib-depleted cells during planar orientation in wing disc epithelial cells. (A and B)** Time-lapse images of dividing wing disc cells expressing Cnn-GFP (green) and His2Av-mRFP (His-RFP; magenta). Representative type 1 (A) and type 2 (B) dividing cells in control wing discs (type 1, *n* = 19/45; type 2, *n* = 26/45). *xy* Projection of *z* stacks (upper panels) and vertical *xz* sections (lower panels). **(C)** To quantify mitotic spindle orientation, θ represents the angle between the spindle axis (line through spindle poles) and the apical plane (*x,y*). **(D)** *Z* rotation dynamics during prometaphase and metaphase for control dividing cells. Each color curve represents an individual mitotic cell (14 representative cells are shown from control, *n* = 45). **(E)** The relative *z* rotation speed for control (*n* = 45), *mud-RNAi* (*n* = 36), and *scrib-RNAi* (*n* = 35) cells. The *z* rotations were measured during the first and second halves of orientation. The expected *z* rotation speed reduction between the first and second halves diminished in *mud-RNAi* and *scrib-RNAi* cells. Error bars are SD. ****, P < 0.0001; n.s., not significant (P > 0.05) by paired two-tailed *t* test. **(F and H)** Time-lapse series of mitotic wing disc cells exhibiting aberrant anaphase spindle orientation for *mud-RNAi* (F) or *scrib-RNAi* (H). **(G and I)** *Z* rotation dynamics during prometaphase and metaphase for *mud-RNAi* (G) or *scrib-RNAi* (I). Random spindle movements were observed in both conditions. Each color curve represents an individual mitotic cell (nine representative cells are shown from each genotype: *mud-RNAi*, *n* = 36; *scrib-RNAi*, *n* = 35). Scale bars: 5 μm.

constructs expressed under the control of the Gal4/upstream activating sequence (UAS) system. We first knocked down *mud* in the wing disc using the *nub-Gal4* driver (*nub-Gal4>mud-RNAi*; HMS01458). Mud-depleted cells were not able to orient their mitotic spindle to the plane of the epithelium and

exhibited random spindle movements (Fig. 1, F and G; Fig. S1 E; and Video 3). While control cells showed a directional bias of spindle movements toward planar orientation during the first half of the orienting process (Fig. 1 D), this directional bias diminished in Mud-depleted cells along with the rotation speed

(Fig. 1 E), resulting in defects in planar spindle alignment (n = 16/36; Fig. S1 J).

We next disrupted Scrib by expressing an RNAi construct targeting *scrib* in the *nub-Gal4* domain (*nub-Gal4>scrib-RNAi*; HMS01490). Importantly, these conditions do not affect epithelial architecture during the normal third-instar larval period (Fig. S2; Nakajima et al., 2013), allowing us to effectively track spindle movements relative to the plane of the epithelium. Interestingly, as with *mud-RNAi*, *scrib*-knockdown cells frequently exhibited random spindle movements and failed to rotate toward planar orientation (Fig. 1, H and I; Fig. S1, F and J; and Video 4; n = 13/35). Furthermore, the directional bias toward planar and phase-dependent changes in rotation speed were not observed in *scrib*-RNAi cells (Fig. 1 E). To examine the role of Dlg while circumventing its requirements for epithelial organization, we used a relatively weak *dlg*-RNAi construct (*nub-Gal4>dlg-RNAi*; JF01365) that does not alter epithelial organization (Fig. S2). Knockdown of *dlg* in the wing disc resulted in a low frequency of spindle misorientation associated with mitotic spindle dynamics similar to those observed in *scrib*-knockdown cells (Fig. S1, G–J; and Video 5; n = 14/102). Although a recent report using fixed samples suggested that Scrib and Dlg do not contribute to planar spindle alignment (Bergstralh et al., 2016), our live imaging results demonstrated that they are required for mitotic spindle movements and planar spindle orientation. These results imply that the junctional tumor suppressors Scrib and Dlg affect mitotic spindle movements in a manner similar to that of Mud, raising a hypothesis that these molecules may function together in the same pathway to control planar spindle alignment.

Junctional localization of Scrib defines the spatial localization of Dlg

During cell division in the wing disc epithelium, Mud accumulates at spindle poles and is also localized at the cell cortex, including the apical junctional region where both Scrib and Dlg accumulate (Fig. 2 A; Nakajima et al., 2013; Bosveld et al., 2016). Although Scrib colocalizes with Dlg at septate junctions (Bilder et al., 2000), how Scrib interacts with Dlg is not clearly understood.

The *Drosophila* Scrib protein contains 16 leucine-rich repeats (LRRs) and four PDZ domains. While the LRR domains are required for epithelial polarity, the PDZ domains contribute to the support of LRR and junction formation (Bilder and Perrimon, 2000). To address the precise requirements for Scrib during planar spindle orientation, we analyzed the hypomorphic alleles *scrib^4* and *scrib^5*, which lack all four PDZ domains and the third and fourth PDZ domains, respectively (Fig. 2 B; Zeitler et al., 2004). It has been suggested that *scrib^4* and *scrib^5* mutant discs exhibit hyperplastic overgrowth but maintain relatively normal apicobasal polarity (Zeitler et al., 2004). We generated mutant clones of *scrib^4* and *scrib^5* using the mosaic analysis with the repressible cell marker (MARCM) method and observed abnormal planar spindle orientation only in *scrib^4* mutant cells (Fig. 2, C and D; and Fig. S3 A). Although overall apico-basal polarity and junctional integrity detected by E-cadherin localization were normal in cells homozygous for both alleles (Fig. 2,

E and F), we found that Dlg localization was clone-autonomously reduced in *scrib^4* mutant cells (Fig. 2, G and H). These results indicate that the effect of Scrib on spindle orientation may be attributed to reduced Dlg localization, which requires the presence of the first and second PDZ domain of Scrib. Overall, these findings suggest that Scrib is required for proper Dlg localization, which is necessary for planar orientation of the mitotic spindle.

A recent report suggests that Dlg regulates the cortical localization of Mud at tricellular junctions, which is necessary for orienting the mitotic spindle along the interphase long axis in the epithelial plane (Bosveld et al., 2016). However, whether tricellular junction proteins are also required for planar spindle orientation remains unclear. Gliotactin (Gli) is the first identified tricellular junction marker in *Drosophila*, and its localization is regulated by Dlg (Schulte et al., 2006; Padash-Barmchi et al., 2013). In addition to Dlg, Gli regulates Mud localization at tricellular junctions (Bosveld et al., 2016), raising the possibility that tricellular junctional localization of Mud controls planar spindle orientation. To address this possibility, we disrupted Gli using two independent RNAi constructs (*nub-Gal4>Gli-RNAi*, HM05262 and HMJ22052; Fig. S3, E–H) and found that mitotic spindles in *Gli*-RNAi wing discs exhibited normal planar orientation (Fig. 3, A and B; and Fig. S3 B). Taken together, these results suggest that Scrib and Dlg control planar spindle orientation by a mechanism distinct from the one used by tricellular junctions.

Scrib/Dlg-mediated spindle orientation does not require the canonical Pins or Hippo pathways

In diverse systems, Dlg controls mitotic spindle orientation through Pins/LGN, which interacts with Gαi anchored at the plasma membrane (Siegrist and Doe, 2005; Saadaoui et al., 2014). A possible role for Pins in planar cell division in the wing disc epithelium has been previously investigated (Guilgur et al., 2012; Dewey et al., 2015). However, more recent work suggests that Pins is not required for the control of planar spindle orientation (Bergstralh et al., 2016). We therefore tested whether or not the canonical Pins pathway has a role in planar division of wing disc epithelial cells. We examined spindle orientation in *pins^p62*-null mutant cells generated using the MARCM technique and confirmed that Pins is dispensable for planar spindle alignment in the wing disc (Figs. 3 C and S3 A). Consistent with the *pins* loss-of-function phenotype, *Gαi^P8*-null mutant cells in the wing disc did not exhibit defects in planar spindle orientation (Figs. 3 D and S3 C). These results support a model wherein the canonical Pins complex is not required for planar spindle alignment in the wing disc epithelium.

In addition to the canonical Pins-mediated machinery, additional reports suggest that the Hippo/Warts kinase pathway controls mitotic spindle orientation in *Drosophila* (Dewey et al., 2015; Keder et al., 2015). Warts phosphorylates Mud in vitro, which leads to the enhancement of the interaction between Pins and Mud, and knockdown of *wts* or *hpo* by RNAi in the wing disc results in abnormal spindle orientation (Dewey et al., 2015). However, our knockdown of *hpo* in the wing disc did not cause defects in planar spindle alignment (*nub-Gal4>hpo-RNAi*,
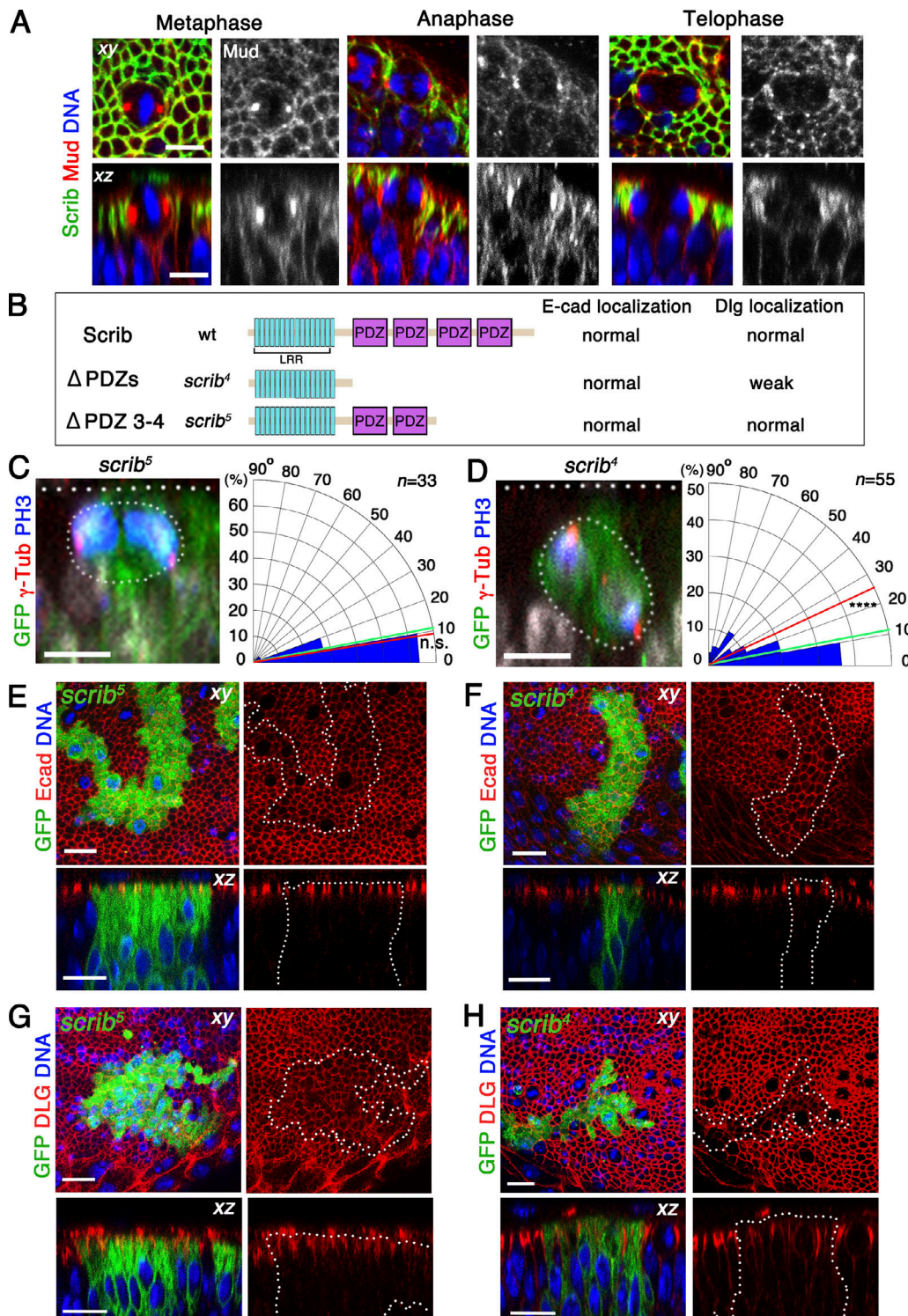
Figure 2. **Scrib PDZ domains are required for the junctional localization of Dlg and planar spindle alignment. (A)** Mud (red) localizes at spindle poles and the cortex during mitosis, including the apical septate junctions as defined by Scrib localization (green). xy Images (upper panels) and xz images (lower panels). **(B)** Domain structure of wild-type Scrib and two mutant forms. The protein product of *scrib⁴* retains only the LRR domains (ΔPDZs). *scrib⁵* retains the LRR domains along with PDZ domains 1 and 2 (ΔPDZ 3–4). E-cad, E-cadherin. **(C and D)** Quantification of mitotic spindle alignment in *scrib⁵* (C) and *scrib⁴* (D) MARCM clones. The red and green lines show the median angular deviation for mutant clones and controls, respectively. *n* indicates the number of spindles observed. *FRT82B* clones (*n* = 33) for control. ****, P < 0.0001; n.s., not significant (P > 0.05) by Kolmogorov–Smirnov test. **(E–H)** E-cadherin and Dlg localization in *scrib⁵* (E and G) and *scrib⁴* (F and H) MARCM clones, respectively. MARCM clones were generated by using *hsFLP UAS-mCD8-GFP; tub-Gal4 FRT82B tub-Gal80/TM6C* with *FRT82* recombined mutant lines. Upper panels are *xy* images; lower panels are cross sections (*xz*). Scale bars: 5 µm (A, C, and D) and 10 µm (E–H).
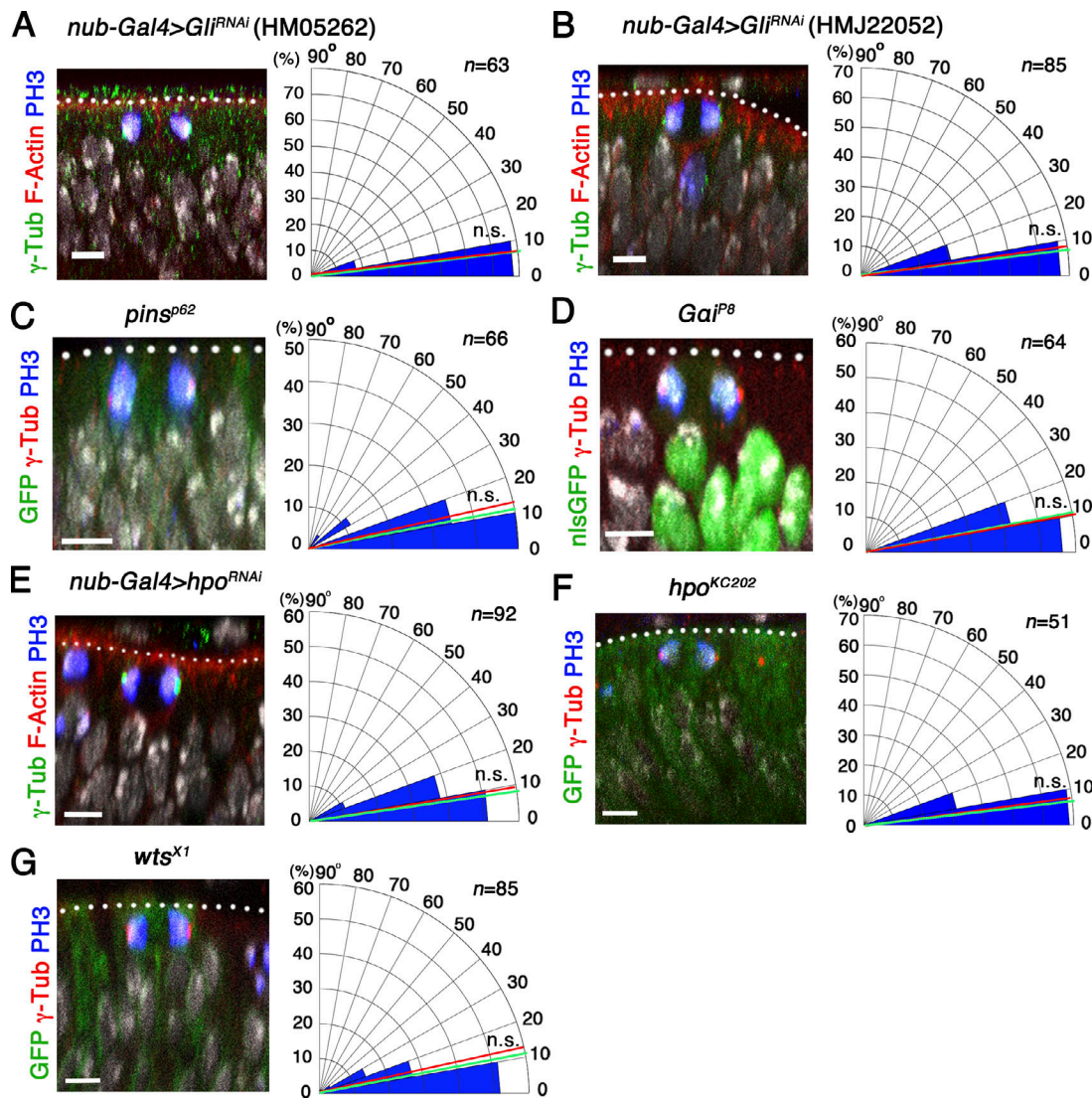
Figure 3. **The canonical Pins and Hippo pathways are not required for planar spindle orientation in the wing disc. (A–G)** Quantification of mitotic spindle alignment in cells expressing *Gli-RNAi* (A and B) and (E) *hpo-RNAi* (*nub-Gal4>RNAi*), as well as *pins^P62* (C), *Gαi^P8* (D), *hpo^KC202* (F), and *wts^X1* (G) MARCM clones. The red and green lines show the median angular deviation for experiments and controls, respectively, and *n* indicates the number of spindles observed. *nub-Gal4* (*n* = 86; A, B, and E), *FRT82B* (*n* = 33; C and G), *FRT2A* (*n* = 70; D), *FRT42D* (*n* = 46; F) for controls (Fig. S3). MARCM clones were generated using *hsFLP UAS-mCD8-GFP; tub-Gal4 FRT82B tub-Gal80/TM6C* (C and G), *yw hsFLP tub-Gal4 UAS-nlsGFP;; tub-Gal80 FRT2A/TM6B* (D), or *hsFLP UAS-mCD8-GFP; FRT42D tub-Gal80; tub-Gal4/TM6B* (F). n.s., not significant. Scale bars: 5 μm.

HMS00006; Figs. 3 E and S3 B). Consistent with this observation, spindle orientation in *hpo^KC202*-null mutant clones did not exhibit abnormality (Figs. 3 F and S3 D). To further test the contribution of the Hippo pathway to planar spindle alignment, we analyzed *wts^X1*-null mutant cell clones and found that planar orientation was not significantly impaired (Figs. 3 G and S3 A). Together, these results indicate that neither the canonical Pins complex nor the Hippo pathway is required for planar spindle alignment in wing disc epithelial cells, suggesting that a Scrib/Dlg-dependent and Pins-independent mechanism operates during this process.

Drosophila 14-3-3 proteins are novel Dlg interaction partners
To identify novel components in the Scrib/Dlg-mediated pathway that controls planar spindle orientation, we used Dlg as a

bait protein and performed proteomic analysis of fly embryonic samples by multidimensional protein identification technology (MudPIT; Florens and Washburn, 2006). From a list of potential Dlg-interacting proteins identified from MudPIT analysis, *Drosophila* 14-3-3 proteins (14-3-3ε/14-3-3ζ) were consistently enriched (Table S1). 14-3-3 proteins are adaptor molecules implicated in diverse aspects of cell division, including cell cycle regulation, maintenance of microtubules, and spindle assembly (Su et al., 2001; Zhou et al., 2010; Freeman and Morrison, 2011; De and Kline, 2013). 14-3-3 proteins were also reported to regulate mitotic spindle orientation in in vitro systems such as 3D culture of mammalian cells (Hao et al., 2010) and an induced-polarity system in *Drosophila* cell culture (Lu and Prehoda, 2013). Intriguingly, the *Drosophila* Interactions Database predicts that 14-3-3 proteins can interact with Mud and the centrosomal

protein Cnn, both of which localize to spindle poles and affect mitotic spindle orientation (Nakajima et al., 2013; Poulton et al., 2014). We therefore hypothesize that the Scrib/Dlg complex may control planar spindle orientation via interaction with 14-3-3 adaptor molecules.

We sought to test whether Dlg and 14-3-3 proteins interact in the context of the wing disc epithelium. We performed coimmunoprecipitation using the Dlg antibody and confirmed the presence of 14-3-3 proteins in the immunoprecipitate of Dlg from wild-type wing disc samples (Fig. 4 A and Fig. S4, A and B). We further conducted an in situ proximity ligation assay (PLA) to examine associations of Dlg and 14-3-3 proteins in the wing disc epithelium (Söderberg et al., 2006). PLA signal spots reflect close proximity or protein–protein interactions, as confirmed by PLA between Scrib and Dlg in the wing disc (Figs. 4 B and S4 C). Notably, PLA signal between Dlg and 14-3-3 was detected at the level of the mitotic zone (Fig. 4 E). This PLA signal was reduced in the mitotic zone of *dlg-RNAi* wing discs (*nub-Gal4>dlg-RNAi*), but not in the peripodial epithelium where *nub-Gal4* was not expressed (Fig. 4, B–G). PLA signal loci were also detected between Scrib and Mud as well as between Mud and 14-3-3 (Fig. S4, D–F). Combined, these results suggest a physical interaction between Scrib, Dlg, Mud, and 14-3-3 proteins in the wing disc epithelium.

We next analyzed the subcellular localization of 14-3-3 proteins in the wing disc epithelium. From both direct immunofluorescence and indirect analysis of exogenously expressed HA-tagged constructs, we found that 14-3-3 proteins are broadly distributed in the cell, featuring localization at the apical cortex and nucleus during interphase, with more cytosolic localization during mitosis, overlapping with both spindle microtubules and the cell cortex (Fig. 4, H and I; and Fig. S5, A–C). By further performing live imaging using a *14-3-3ε-GFP* protein trap line, we confirmed diffuse localization with enrichment at the apical cortex during interphase followed by a broader cytosolic redistribution of 14-3-3ε-GFP during mitosis and its striking concentration in the midbody during cytokinesis (Fig. S5, D–F; and Video 6). The close association of 14-3-3 proteins with spindle microtubules may reflect their interaction. Indeed, a recent report provides evidence that 14-3-3 proteins locally activate spindle proteins in the *Drosophila* oocyte during meiosis (Beaven et al., 2017).

14-3-3 proteins are required for planar spindle alignment in wing disc epithelial cells

The dynamic localization of 14-3-3 proteins during mitosis could reflect their functional requirement during cell division. To examine the role of 14-3-3 proteins in the developing wing disc, we generated homozygous mutant clones for the loss-of-function alleles of *14-3-3ε^{j2B10}* or *14-3-3ζ^{12BL}* with the MARCM method. We observed subtle but significant defects in spindle orientation in *14-3-3ε^{j2B10}* mutant cells (Fig. 5 A) but did not observe abnormal spindle orientation in *14-3-3ζ^{12BL}* mutant cells (Fig. 5 B). Because 14-3-3 proteins are known to work as heterodimers (Gardino and Yaffe, 2011) and *Drosophila* 14-3-3ε and 14-3-3ζ have been shown to interact directly (Lu and Prehoda, 2013), it is possible that both 14-3-3 proteins could function either together

or redundantly in controlling planar spindle orientation. To probe this possibility, we analyzed *14-3-3ε^{j2B10}* mutant cells in a *14-3-3ζ^{12BL}* heterozygous background (*14-3-3ζ^{12BL}/+, 14-3-3ε^{j2B10}*). Strikingly, in *14-3-3ζ^{12BL}/+, 14-3-3ε^{j2B10}* cells, spindle orientation became nearly random (Fig. 5 C). Furthermore, by targeting *14-3-3ζ* with expression of an RNAi-construct in *14-3-3ε^{j2B10}* mutant cells (*14-3-3ζ-RNAi, 14-3-3ε^{j2B10}*), we also observed severe defects in spindle orientation (Fig. 5 D). Importantly, these *14-3-3* mutant cells in the epithelial layer do not lose epithelial polarity or junctional integrity (Fig. 5, E and F). Although 14-3-3 proteins are likely to play diverse additional roles in cellular homeostasis (Le et al., 2016), these results support the idea that 14-3-3 proteins cooperatively regulate proper spindle orientation in the wing disc epithelium.

As shown previously, a consequence of spindle misorientation in the wing disc epithelium is basal cell delamination, followed by apoptotic cell death (Guilgur et al., 2012; Nakajima et al., 2013; Poulton et al., 2014). We examined wing discs containing *14-3-3ζ^{12BL}/+, 14-3-3ε^{j2B10}*, or *14-3-3ζ-RNAi, 14-3-3ε^{j2B10}* mutant cell clones and found a significant increase of apoptotic cells located at the basal side of the epithelium (Fig. 5, G and H). Consistent with an increase of apoptotic cells, after suppressing cell death by expressing the caspase inhibitor *p35*, we observed abnormal mesenchyme-like cell masses on the basal surface of the epithelium (Fig. 5, I and J). These tumor-like cell masses constitute a feature of the enforced survival of misaligned cells from the wing disc epithelium (Nakajima et al., 2013; Poulton et al., 2014; Muzzopappa et al., 2017). Together, these results suggest that 14-3-3 proteins are required for proper control of planar spindle alignment during wing disc growth and thus contribute to the maintenance of epithelial architecture by suppressing basal cell delamination via aberrant cell divisions.

To further verify a functional link between 14-3-3 proteins and the Scrib/Dlg-mediated pathway, we tested for genetic interactions. Double knockdown of *mud* and *14-3-3ε* showed an additive effect on spindle misorientation to an extent similar to that of double knockdown of *mud* and *scrib* (Fig. 6 A). We also used the *14-3-3ε^{j2B10}* heterozygous background to concomitantly knock down genes with *nub-Gal4>UAS-RNAi*. Although deleting one copy of *14-3-3ε* did not affect spindle orientation on its own, simultaneous knockdown of either *mud* or *scrib* induced more severe spindle-orientation defects than single depletion of either gene, suggesting a genetic interaction between *scrib, mud*, and *14-3-3ε* (Fig. 6 A). No such increase in spindle orientation defects was observed in *pins* heterozygous background or in knockdown of *pins* in the *mud-RNAi* wing disc (Fig. 6 A). The fact that reducing *14-3-3ε* gene dosage in *scrib* and *mud* RNAi backgrounds enhances spindle orientation defects implies that 14-3-3ε contributes to the control of planar spindle alignment in the wing disc epithelium with septate junction–associated proteins and Mud.

Finally, we investigated potential molecular connections between Scrib, Dlg, 14-3-3s, and Mud. Because 14-3-3 proteins physically interact with Dlg, and Scrib/Dlg and Mud control mitotic spindle movement, our findings suggest a model in which 14-3-3s and Mud could detect Scrib and Dlg as cortical cues and use them to achieve planar alignment. To test this
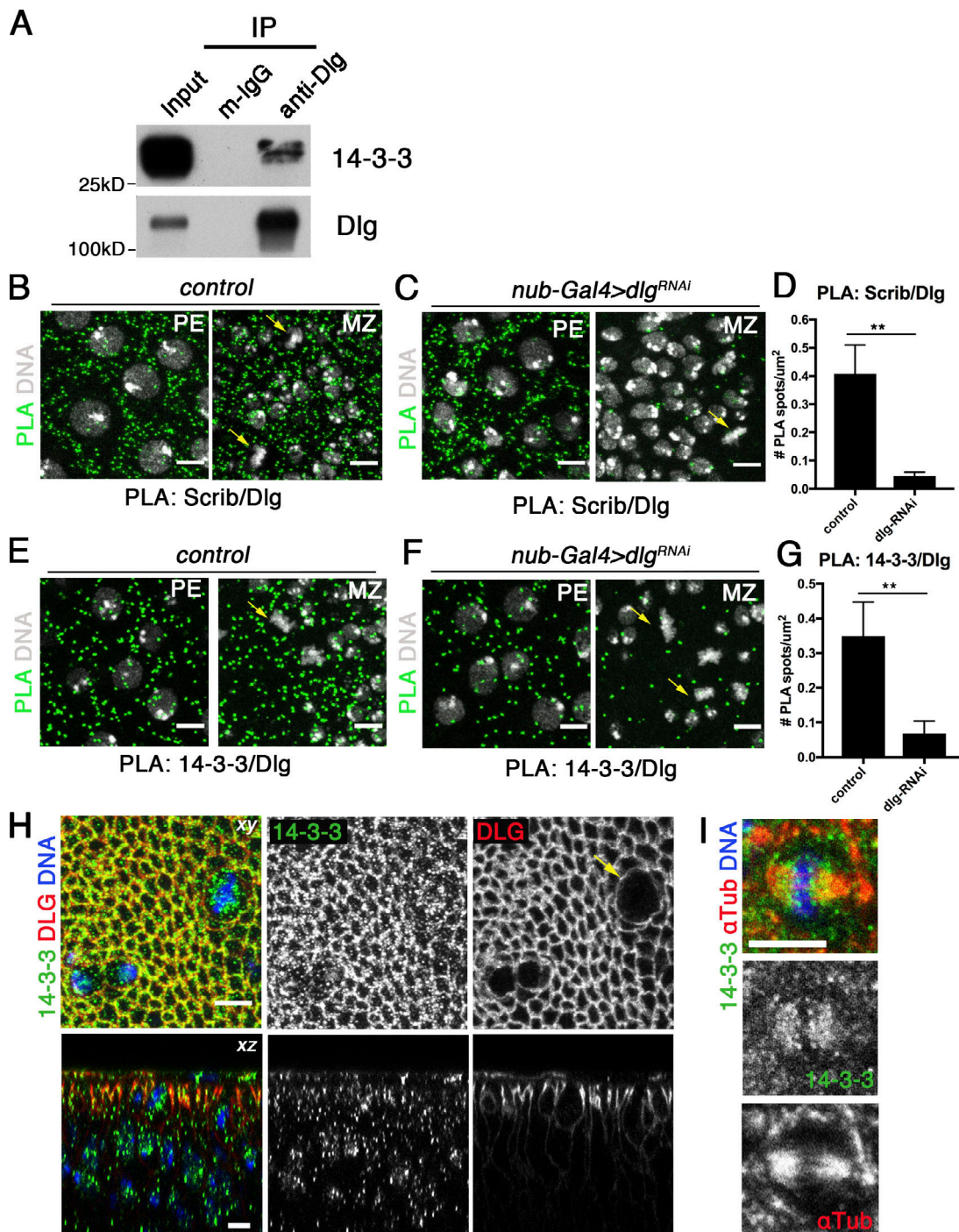
Figure 4. **_Drosophila_ 14-3-3 proteins interact with Dlg in the wing disc epithelium. (A)** Coimmunoprecipitation of endogenous 14-3-3 proteins and Dlg from wild-type wing disc samples. Western blots were probed with anti–14-3-3 antibody (upper lanes) and anti-Dlg antibody (lower lanes) in input and immunoprecipitates pulled down by anti-Dlg antibody. IP, immunoprecipitation. **(B–G)** PLA indicates close proximity or interactions of two proteins. PLA between Scrib and Dlg in control (_nub-Gal4/+_; B) and _dlg_-knockdown (_nub-Gal4>dlg-RNAi_; C) wing discs. **(D)** Quantification of the number of PLA (Scrib/Dlg) spots for control (_n_ = 6) and _dlg-RNAi_ (_n_ = 5) wing discs. PLA between 14-3-3 and Dlg in control (E) and _dlg_-knockdown (F) wing discs. **(G)** Quantification of the number of PLA (14-3-3/Dlg) spots for control (_n_ = 5) and _dlg-RNAi_ (_n_ = 5) wing discs. Error bars are SD. **, P < 0.01 by Kolmogorov–Smirnov test. Note that PLA signals in MZ of the disc proper diminished in _dlg_-RNAi wing discs, but not in PE where _nub-Gal4_ is not expressed. PE, peripodial epithelium; MZ, mitotic zone. **(H and I)** Subcellular localization of 14-3-3 proteins detected by anti–14-3-3 antibody staining. 14-3-3 proteins localize to the apical cortex and nucleus during interphase (H) and cytosol, including spindle microtubules (α-tubulin), during mitosis (I). Yellow arrows indicate metaphase cells. Scale bars: 5 µm.

Nakajima et al.
Scrib/Dlg/14-3-3 control planar spindle alignment

Journal of Cell Biology
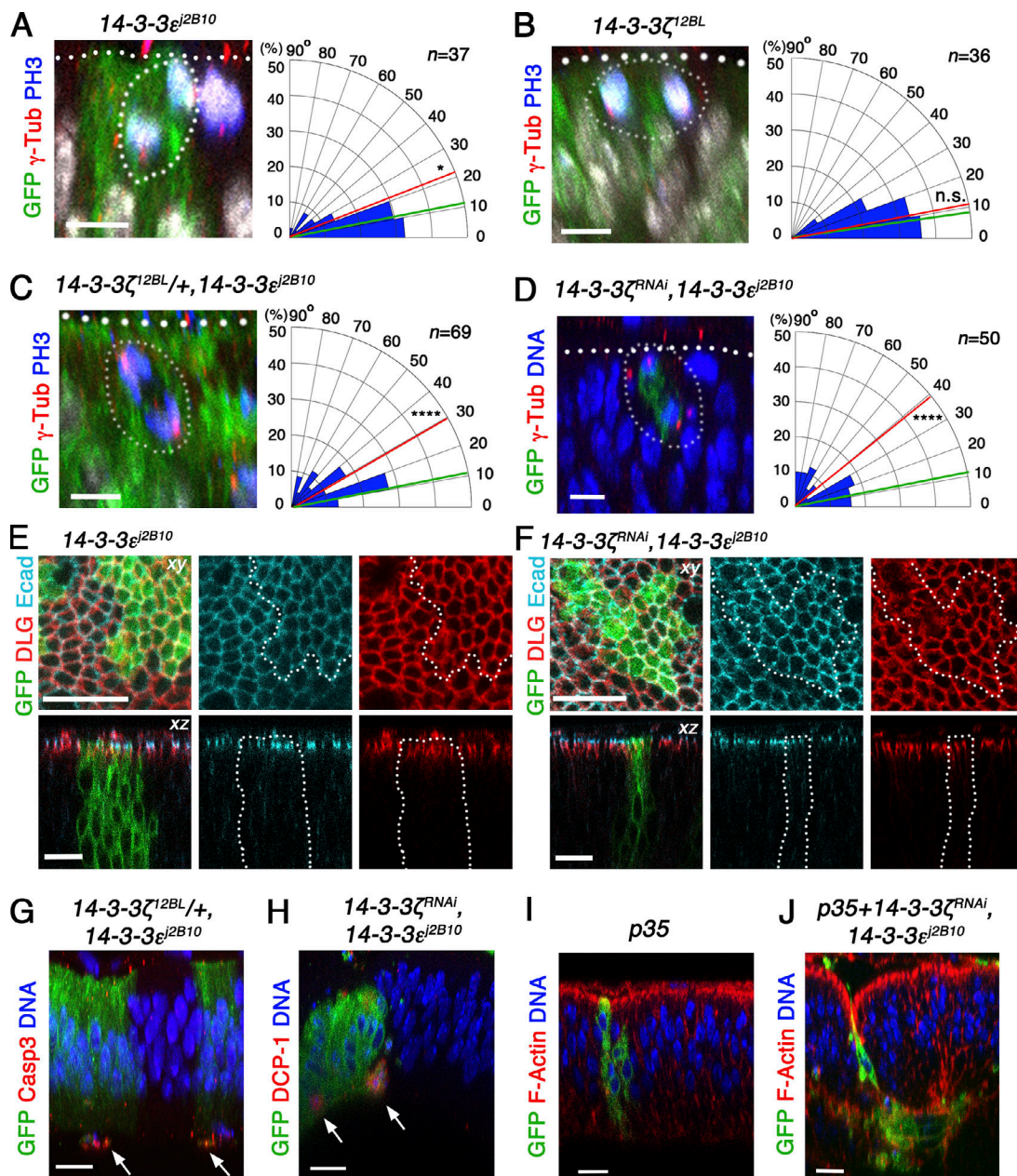https://doi.org/10.1083/jcb.201803116

1831

Figure 5. **14-3-3 proteins are required for planar spindle alignment in wing disc epithelial cells. (A–D)** Quantification of mitotic spindle alignments in *14-3-3ε^{j2B10}* (A) and *14-3-3ζ^{12BL}* (B) MARCM clones, as well as in *14-3-3ε^{j2B10}* (C) MARCM clones in a *14-3-3ζ^{12BL}* heterozygous background (*14-3-3ζ^{12BL}/+, 14-3-3ε^{j2B10}*) and with coexpression of *14-3-3ζ-RNAi* (VDRC48724; *14-3-3ζ-RNAi, 14-3-3ε^{j2B10}*; D). The red line shows the median angular deviation for each mutant condition compared with controls (green). *n* indicates the number of spindles observed. FRT82B (*n* = 33; A, C, and D), FRT42D (*n* = 46; B) for controls. *, P = 0.0171; ****, P < 0.0001; n.s., not significant (P > 0.05) by Kolmogorov–Smirnov test. **(E and F)** E-cadherin and Dlg localization in *14-3-3ε^{j2B10}* (E) and *14-3-3ζ-RNAi, 14-3-3ε^{j2B10}* (F) MARCM clones, respectively. Upper panels are *xy* images; lower panels are cross sections (*xz*). **(G and H)** Depletion of 14-3-3 proteins in wing discs induces basal cell delamination associated with apoptosis. Apoptotic cells (arrows) are labeled by anti–cleaved caspase 3 or anti–cleaved death caspase 1 (DCP-1) staining in MARCM clones of *14-3-3ζ^{12BL}/+, 14-3-3ε^{j2B10}* (G) and *14-3-3ζ-RNAi, 14-3-3ε^{j2B10}* (H). **(I)** Control MARCM clones expressing *p35*. **(J)** *14-3-3ε^{j2B10}* MARCM clones expressing *p35* with *14-3-3ζ-RNAi* exhibit mesenchymal-like morphology. MARCM clones were generated by using *hsFLP UAS-mCD8-GFP; tub-Gal4 FRT82B tub-Gal80/TM6C* (A and C–J) or *hsFLP UAS-mCD8-GFP; FRT42D tub-Gal80; tub-Gal4/TM6B* (B). Scale bars: 5 μm (A–D) and 10 μm (E–J).

model, we applied the PLA method to genetic perturbations using *nub-Gal4>UAS-RNAi*. Consistent with our model, when Dlg was disrupted by RNAi in the wing disc, the number of loci showing PLA signal between Scrib and Mud significantly decreased (Fig. 6, B, C, and E), Similarly, we observed a significant decrease in PLA-positive foci between Scrib and Mud in *14-3-3-RNAi*

wing discs where both 14-3-3 proteins were knocked down (Fig. 6, B, D, and E), while PLA signal between Scrib and Dlg was not affected (Fig. S4, G–I). Based on these results, we propose a model wherein 14-3-3 proteins could function as a molecular bridge between Dlg and the mitotic apparatus organized by Mud during planar division of the wing disc epithelial cells (Fig. 6 F).
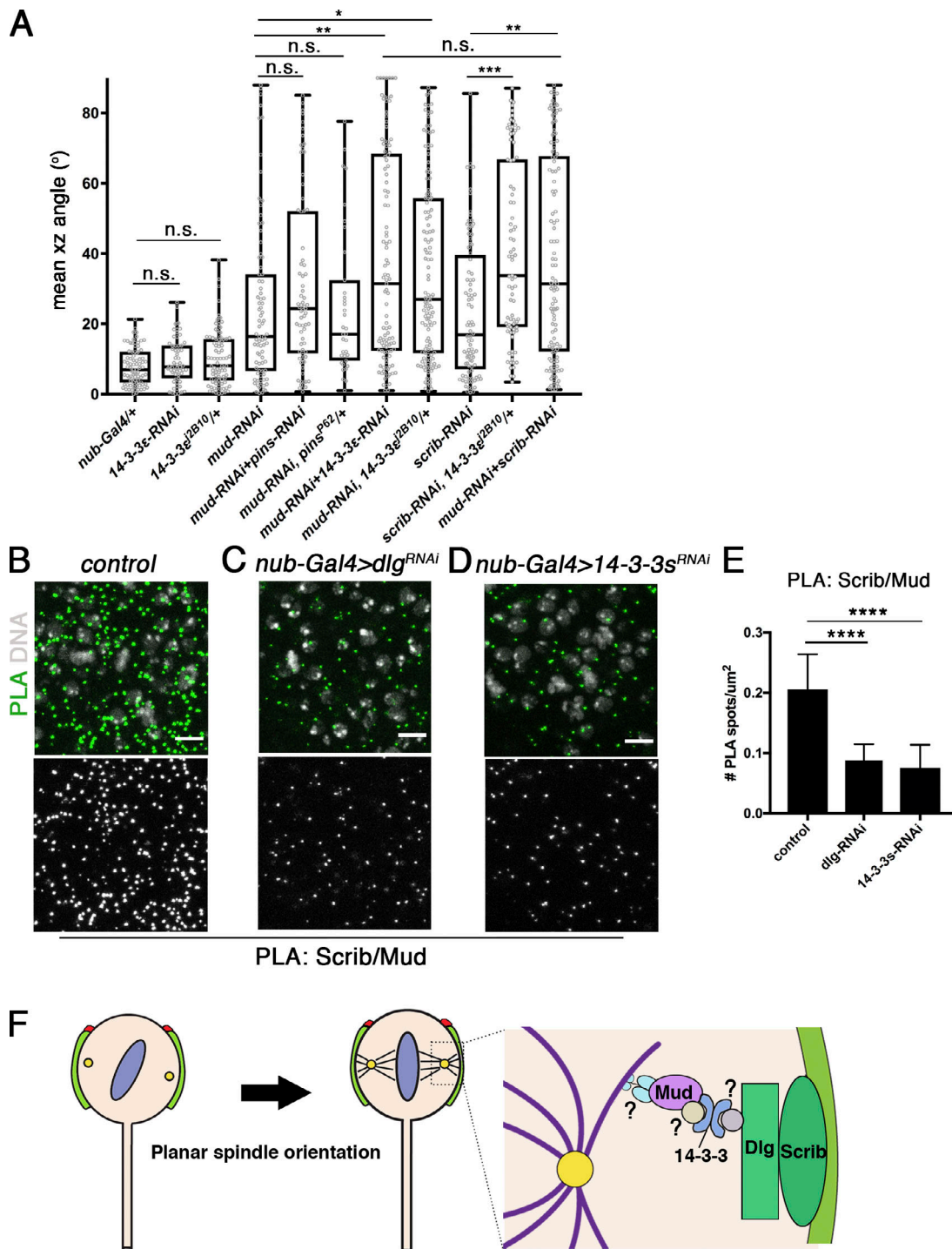
Figure 6. **14-3-3 proteins genetically interact with Scrib and Mud and function as a molecular bridge between Dlg and Mud.** **(A)** Quantification of mitotic spindle alignments in different genetic backgrounds. Knockdown of *14-3-3ε* alone or the *14-3-3ε^{j2B10}* heterozygous background alone (*14-3-3ε^{j2B10}/+*) did not affect planar spindle orientation. Reduction of *14-3-3ε* levels by *14-3-3ε-RNAi* (HMS01229) or *14-3-3ε^{j2B10}/+* in *mud-RNAi* or *scrib-RNAi* discs significantly increased abnormal spindle orientation, while reduction of *pins* levels by *pins-RNAi* (HMS01462) or *pins^{P62}/+* in *mud-RNAi* did not. Data are shown as box plots (median ± quartiles). Each point represents a cell. *, P < 0.01; **, P < 0.001; ***, P < 0.0001; n.s., not significant (P > 0.05) by Kolmogorov–Smirnov test. The number of analyzed spindles is as follows: *nub-Gal4/+*, n = 86; *14-3-3ε-RNAi*, n = 58; *14-3-3ε^{j2B10}/+*, n = 83; *mud-RNAi*, n = 83; *mud-RNAi+pins-RNAi*, n = 73; *mud-RNAi+pins^{P62}/+*, n = 35; *mud-RNAi+14-3-3ε-RNAi*, n = 109; *mud-RNAi+14-3-3ε^{j2B10}/+*, n = 128; *scrib-RNAi*, n = 92; *scrib-RNAi +14-3-3ε^{j2B10}/+*, n = 68; and *mud-RNAi+scrib-RNAi*, n = 114. **(B–D)** PLA between Scrib and Mud in control (*nub-Gal4/+*; B), *dlg*-knockdown (C *nub-Gal4>dlg-RNAi*; C), and *14-3-3ζ/14-3-3ε*-knockdown (*nub-Gal4>14-3-3s-RNAi* as *14-3-3ε-RNAi* and *14-3-3ζ-RNAi* from Ren et al., 2010; D) wing discs. **(E)** Quantification of the number of PLA (Scrib/Mud) spots for control (n = 15), *dlg-RNAi* (n = 12), and *14-3-3s-RNAi* (n = 16) wing discs. Error bars are SD. ****, P < 0.0001 by Kolmogorov–Smirnov test. Scale bars: 5 μm. **(I)** Model illustrating how junctional proteins Scrib and Dlg may control planar spindle orientation by interacting with 14-3-3 proteins. 14-3-3 proteins could work as a molecular link between Dlg and Mud, which in turn interact with microtubules (purple) and motor proteins (cyan). Adherens junctions (red), septate junctions (green), spindle poles (yellow), and potential interacting proteins (small circles).

Discussion

This study uncovers a novel function for 14-3-3 proteins in controlling planar spindle alignment mediated by the junction-localized proteins Scrib and Dlg. Together with Mud, Scrib and Dlg regulate mitotic spindle movements during prometaphase and metaphase, and defects in this process can lead to aberrant spindle orientation. We present further evidence that Dlg localization depends on the Scrib PDZ domains, which are also necessary for planar spindle orientation. Finally, based on biochemical and genetic interactions, we propose that 14-3-3 proteins provide a molecular link between Dlg and the mitotic apparatus to control planar spindle alignment (Fig. 6 F).

Recent studies have listed several polarity and junctional molecules as regulators of planar spindle orientation; however, their exact roles in cellular processes in vivo, including dynamic spindle movements, remain elusive. In this study, using live-imaging analysis, we revealed biphasic spindle movements accompanying a directional bias toward planar orientation during wing disc cell division (Fig. 1, D and E). RNAi-mediated knockdown of *scrib* or *dlg* in the developing wing disc caused random spindle movements without affecting apico-basal polarity, as observed in *mud*-RNAi wing discs (Fig. 1, E–I; Fig. S1, G–I; and Fig. S2), suggesting that junctional proteins Scrib and Dlg control spindle rotation and restrict spindle positioning in the epithelial plane. Such biphasic spindle movements are controlled by the Gαi/LGN/NuMA complex during planar division in the chick neuroepithelium (Peyre et al., 2011). Together, these results suggest that, although distinct molecular mechanisms are used, a conserved spindle movement program underlies planar spindle orientation in epithelia across different species.

As Scrib and Dlg stay localized to the cortex during mitosis, these junctional proteins could function together as a molecular cue to orient the mitotic spindle. Scrib and Dlg often function with Lethal giant larvae (Lgl), a *Drosophila* neoplastic tumor suppressor that localizes to the basolateral cortex during interphase. In both the follicular epithelium and the wing disc epithelium, Lgl exhibits cytoplasmic relocalization during mitosis, which has been suggested to promote planar spindle orientation (Bell et al., 2015; Carvalho et al., 2015). Mechanistically, Lgl cortical release can remodel the Dlg/Lgl complex at the cortex, allowing Dlg to interact with Pins. However, recent work, together with this study, suggests that neither the removal of Lgl from the cortex nor the canonical Pins pathway is necessary for planar spindle orientation in the wing disc epithelium (Fig. 3; Bergstralh et al., 2016). These observations raise the following questions: how could Scrib/Dlg molecularly control mitotic spindle orientation in a Pins-independent manner, and how much conservation and diversification exist between planar orientation machineries?

Dlg is an evolutionarily conserved scaffold protein that regulates diverse aspects of cellular processes including adhesion, polarity, and spindle orientation (Anderson et al., 2016). With N-terminal PDZ domains and a C-terminal guanylate kinase domain, Dlg can bind to both cortical proteins and motor proteins, such as Pins and Khc-73, respectively (Johnston et al., 2009). In columnar-shaped *Drosophila* wing disc cells, septate junctions are mature, and septate junction–associated proteins accumulate near the apical epithelial surface where mitotic spindles align (Meyer et al., 2011). As shown in this study, septate junction–localized Scrib regulates the proper localization of Dlg, which controls planar spindle alignment in a Pins-independent manner (Fig. 2). By contrast, in the cuboidal-shaped *Drosophila* follicle cells, despite the lack of septate junctions during proliferative stages, mitotic spindles orient to the lateral cortex where septate junction–associated proteins localize (Bergstralh et al., 2013; Carvalho et al., 2015). Accordingly, Dlg at the lateral cortex restricts Pins localization to control planar cell division, similar to the mechanism used in the chick neuroepithelium (Bergstralh et al., 2013; Saadaoui et al., 2014). It is thus tempting to speculate that the cortical localization of Dlg is a conserved feature that provides a spatial cue for dividing epithelial cells by associating with different proteins to orient mitotic spindles, depending on epithelial cell characteristics and maturity.

Our study is the first to demonstrate the requirement of 14-3-3 proteins for planar spindle alignment during epithelial cell division in vivo. In contrast to in vitro cell culture studies implicating 14-3-3 proteins in the Pins-mediated spindle orientation machinery (Hao et al., 2010; Lu and Prehoda, 2013), we propose a novel mechanism by which 14-3-3 proteins interact with junctional proteins to orient the mitotic spindle. We provide evidence that 14-3-3 proteins physically interact with Dlg (Fig. 4), although the direct or indirect nature of in vivo protein–protein interaction remains to be elucidated. Because 14-3-3 proteins change their localization from the cortex and nucleus during interphase to the cytoplasm during mitosis (Fig. 4, H and I; and Fig. S5), one possibility is that 14-3-3 proteins interact with motor proteins to control mitotic spindle orientation. Indeed, in *Drosophila* S2 cells, the 14-3-3ε/14-3-3ζ heterodimer interacts with the kinesin Khc-73 and a dynein cofactor NudE (Lu and Prehoda, 2013). The cytoplasmic dynein fraction, light intermediate chain 2, interacts with both 14-3-3ε and 14-3-3ζ in HeLa cells (Mahale et al., 2016). A critical next step will be to identify additional interacting players involved in 14-3-3–mediated spindle orientation in vivo.

We propose that 14-3-3 proteins could function as a molecular link that connects the junction-associated proteins Scrib/Dlg and the mitotic apparatus (Fig. 6 F). This model is supported by the finding that knockdown of both *14-3-3s* or *dlg* results in the reduction of physical associations between Scrib and Mud (Fig. 6, B–E). We further show genetic interactions among 14-3-3s, Scrib, and Mud that affect planar spindle orientation (Fig. 6 A). Combined, our data suggest that 14-3-3s function together with Scrib and Dlg to control planar spindle alignment, providing a new insight into the control of tissue growth and homeostasis regulated by these neoplastic tumor suppressors. Given that Scrib and Dlg are conserved molecules involved in cell and tissue polarity and are implicated in epithelial diseases, future work should assess whether the same machinery controls mitotic spindle orientation in vertebrates and across diverse epithelial contexts.

Materials and methods

Fly stocks and genetics

The following stocks were used: *His2Av-mRFP* (Pandey et al., 2005); *UAS-Cnn-GFP* (Megraw et al., 2002); *14-3-3ε-GFP*

Nakajima et al.
Scrib/Dlg/14-3-3 control planar spindle alignment

Journal of Cell Biology   1834
https://doi.org/10.1083/jcb.201803116

(G00082; Morin et al., 2001); Dlg–GFP (CC01936) and *Scrib-GFP* (CA07683; Buszczak et al., 2007); *UAS-HA-14-3-3ε, UAS-HA-14-3-3ζ, UAS-14-3-3ε-RNAi,* and *UAS-14-3-3ζ-RNAi* (Ren et al., 2010); *UAS-Dcr-2; nub-Gal4, UAS-mud-RNAi* (HMS01458), *UAS-scrib-RNAi* (HMS01490), *UAS-dlg-RNAi* (JF01365), *UAS-14-3-3ε-RNAi* (HMS01229), *UAS-hpo-RNAi* (HMS00006), *UAS-Gli-RNAi* (HM05262; HMJ22052), *UAS-pins-RNAi* (HMS01462), *UAS-14-3-3ζ-RNAi* (VDRC48724), and *UAS-p35, hsFLP UAS-mCD8-GFP; tub-Gal4 FRT82B tub-Gal80/TM6C, hsFLP UAS-mCD8:GFP; FRT42D tub-Gal80; tub-Gal4/TM6B, yw hsFLP tub-Gal4 UAS-nlsGFP;; tub-Gal80 FRT2A/ TM6B* for MARCM clones; *FRT82B, FRT2A, FRT42D, w^{1118},* and *14-3-3ε^{j2B10}* (Chang and Rubin, 1997); *14-3-3ζ^{12BL}* (Broadie et al., 1997); *scrib⁴* and *scrib⁵* (Zeitler et al., 2004); *pins^{p62}* (Yu et al., 2000); *Gαi^{P8}* (Yu et al., 2003); *hpo^{KC202}* (Udan et al., 2003); and *wts^{X1}* (Xu et al., 1995). Larvae were raised and collected at 25°C. MARCM mutant clones (Lee and Luo, 1999) were generated with a 1-h heat shock between 48 and 72 h after egg lay, except for the *14-3-3ζ-RNAi, 14-3-3ε^{j2B10}* mutant, in which a 1-h heat shock was induced between 96 and 108 h after egg lay.

Immunofluorescence and image analysis

The following antibodies and dyes were used for fixed tissue imaging: rabbit anti–phospho-Histone H3 (1:1,000; 06-570; Millipore), mouse anti–phospho-Histone H3 (1:2,000; 05-806; Millipore), mouse anti–γ-tubulin (1:1,000; T6557; Sigma-Aldrich), mouse anti–α-tubulin (1:1,000; T9026; Sigma-Aldrich), rabbit anti–cleaved caspase-3 (1:500; 9661; Cell Signaling Technology), rabbit anti–cleaved death caspase-1 (Asp216; 1:200; 9578; Cell Signaling Technology), mouse anti-Mud (1:50; F. Matsuzaki, RIKEN, Kobe, Japan), rabbit anti-Scrib (1:5,000; C. Doe, University of Oregon, Eugene, OR), mouse anti-Gli (1:100; V. Auld, The University of British Columbia, Vancouver, Canada), mouse anti-Dlg (1:200; 4F3; Developmental Studies Hybridoma Bank), rat anti-ECAD (1:50; DCAD2; Developmental Studies Hybridoma Bank), rabbit anti–14-3-3 (1:200; 51-0700; Invitrogen), rat anti-HA (1:200; 3F10; Roche), fluorescent secondary antibodies 488, 555, and 647 (1:500; Invitrogen), Alexa Fluor Phalloidin 488 and 546 (1:500; Invitrogen), and Hoechst 33342 (2 µM; Thermo Fisher Scientific). Confocal images were collected with a 63× 1.30-NA glycerol or 40× 1.25-NA oil objective lens on an SP5 AOBS confocal microscope system (Leica Microsystems).

For quantification of polarity and junctional marker proteins in *scrib* or *dlg*-RNAi wing discs in Fig. S2, projection images of the series of cross sections (xz image) were used (projection of 10 slices, 1 µm per slice). The fluorescent intensity of aPKC or E-cadherin antibody staining along the apical surface of the wing disc (pouch, the first fold, and the second fold) was measured using Fiji.

For mitotic spindle orientation measurement, we followed the procedure described previously (Nakajima et al., 2013). For the live imaging of ex vivo–cultured wing discs, detailed steps of mounting procedures were described in a previous report (Ragkousi et al., 2017). Wing discs were dissected in PBS and cultured in fly medium in which 2% FBS (Gibco) and 0.5% penicillin-streptomycin (Gibco) were added in Shields and Sang M3 Insect Medium (Sigma-Aldrich); time-lapse images were

collected with a 63× 1.20-NA water objective lens at 1- or 2-min intervals.

Semiautomated spindle movement analysis

Time series of individual wing discs were analyzed in Imaris (Bitplane). For each pair of centrosomes, a "Spots" object was created, and each centrosome was tracked manually from just before arrival at the top of the epithelium to the time point just after division. 3D vision glasses were used to verify Imaris's selection of the brightest z position for the point selected. Dividing cells were chosen such that the z axis of the microscope was perpendicular to the plane of the epithelium at that point, corresponding generally to the central region of the disc. Track positions, converted to micrometers in Imaris, were exported and processed in Matlab (MathWorks). There, individual tracks were converted to displacements for each time point: $\Delta\vec{r}_t = \vec{r}_{C1,t} - \vec{r}_{C2,t}$. Next, the angle relative to the epithelium was calculated using Matlab's Cartesian to spherical coordinate system formula and converted to degrees:

$$Angle = \frac{atan2\left(\Delta r_z, \sqrt{\Delta r_x^2 + \Delta r_y^2}\right)}{\pi} \times 180°.$$

Trajectories were then plotted, synchronizing the time point at which centrosomes became visible.

Preparation of protein complexes from fly embryos

Fly embryos (*w^{1118}, Dlg-GFP,* or *Scrib-GFP*) were lysed with lysis buffer (25 mM Tris-HCl, 150 mM EDTA, 1% NP-40, 5% glycerol, 1 mM DTT, and 1× protease inhibitor). Debris was removed by centrifugation, and extracts were preincubated with Dynabeads Protein G (Invitrogen) for 1 h to reduce nonspecific binding to the beads. Immunocomplexes were formed by incubation for 2 h with Dlg antibody–conjugated magnetic beads or GFP-nanobody (GFP-Trap_MA; ChromoTek). Immunocomplexes were washed with wash buffer (25 mM Tris-HCl and 150 mM EDTA), eluted with elution buffer (50 mM glycine, pH 2.5, and 150 mM NaCl), and then neutralized with Tris-HCl, pH 9.5. Two biological replicates of Dlg immunoprecipitations (and their corresponding negative controls without antibody) and two GFP immunoprecipitations from flies expressing either Dlg-GFP or Scrib-GFP (and their negative GFP immunoprecipitation control) were analyzed by MudPIT mass spectrometry (Florens and Washburn, 2006).

MudPIT analysis

TCA-precipitated protein eluates were urea denatured, reduced, alkylated, and digested with endoproteinase LysC followed by trypsin. The peptide mixtures were loaded onto microcapillary fused silica columns (100-µm internal diameter), placed in-line with an Agilent 11000 quaternary pump, and analyzed by a 10-step MudPIT on linear ion traps. Tandem mass spectrometry datasets were searched using SEQUEST (Eng et al., 1994) against a *Drosophila* database (National Center for Biotechnology Information, 2012-03-08 release) containing 18,564 nonredundant proteins and 177 usual contaminants (human keratins, IgGs, and proteolytic enzymes). To estimate false discovery rates, the

amino acid sequence of each nonredundant protein was randomized and searched at the same time. Peptide/spectrum matches were sorted and selected using DTASelect (Tabb et al., 2002) with the following criteria set: spectra/peptide matches were retained only if they had a DeltCn of ≥0.8, and minimum XCorr of 1.8 for singly, 2.5 for doubly, and 3.5 for triply charged spectra. Additionally, the peptides had to be a minimum of seven amino acids in length and fully tryptic. The false discovery rates were 0.5 ± 0.3 and 1.3 ± 0.8 at the peptide and protein levels, respectively. Peptide hits from multiple runs were compared using CONTRAST (Tabb et al., 2002). Distributed normalized spectral abundance factors were used to estimate relative protein levels (Zhang et al., 2010). Proteins significantly enriched in the three Dlg replicate immunoprecipitations but not in control samples (Table S1) were determined using the Power Law Global Error Model signal-to-noise method (Pavelka et al., 2008). The mass spectrometry dataset has been deposited to the ProteomeXchange (http://www.proteomexchange.org/; Vizcaíno et al., 2014) and is available with accession number PXD011016.

Immunoprecipitation

1,200 wing discs were dissected from third-instar larvae and homogenized in chilled lysis buffer (10 mM Tris-HCl, pH 7.5, 150 mM NaCl, 0.5 mM EDTA, and 0.5% NP-40), supplemented with 1× protease (cOmplete tablets, mini EDTA-free; Roche) and phosphatase (PhosSTOP; Roche) inhibitors. The extract was spun at 14,000 g at 4°C for 15 min. 10% of the lysate was removed for the input. The lysate was halved and incubated with either mouse anti-Dlg (1 µg; 4F3; Developmental Studies Hybridoma Bank) or mouse IgG1 isotype control (1 µg; 5415; Cell Signaling Technology) conjugated Dynabeads Protein G (Invitrogen) cross-linked with BS[3] (Invitrogen) at 4°C overnight, with rotation. Beads were then washed three times in lysis buffer and eluted in 30 µl of 2× sample buffer (50 mM Tris-HCl, pH 6.8, 2% SDS, 10% glycerol, 12.5 mM EDTA, and 0.02% Bromophenol Blue) at 70°C for 10 min. Eluted proteins were denatured at 95°C for 5 min with 12.5 mM DTT before Western blotting.

Western blotting

Indicated samples were fractionated by SDS-PAGE gel electrophoresis in mini-PROTEAN 4–20% gradient gels (Bio-Rad). Protein was transferred to PVDF according to the manufacturer's protocols (Bio-Rad). After blocking with 5% nonfat milk in TBST (10 mM Tris, pH 8.0, 150 mM NaCl, and 0.5% Tween 20) for 1 h, the membrane was probed with primary antibodies, rabbit anti–14-3-3 pan (1:200; 51-0700; Invitrogen) and mouse anti-Dlg (1:1,000; 4F3; Developmental Studies Hybridoma Bank). Secondary HRP-conjugated antibodies, goat anti-rabbit (1:10,000; 111-035-003; Jackson ImmunoResearch) and goat anti-mouse (1:10,000; A10668; Invitrogen), were used for detection using SuperSignal West Dura (Thermo Fisher Scientific). Blots were exposed to film (Hyperfilm MP; GE Healthcare) to generate images using a film processor (X-OMAT 200A; Kodak).

In situ PLA

In situ PLA was performed using the Duolink In Situ PLA reagents (Sigma-Aldrich) and with slight modifications to the

manufacturer's protocol (https://www.sigmaaldrich.com/technical-documents/protocols/biology/duolink-fluorescence-user-manual.html#fluorescence). Dissected larval carcasses including wing discs were fixed with 4% PFA, washed with PBT (PBS with 0.1% Triton X-100) three times for 20 min each, and blocked with the Duolink Blocking Solution for 30 min at 37°C. The carcasses were incubated with primary antibodies against two proteins of interest in PBT overnight at 4°C. The following antibodies were used: mouse anti-Dlg (1:200; 4F3; Developmental Studies Hybridoma Bank), mouse anti-Mud (1:50; F. Matsuzaki), rabbit anti-Scrib (1:5,000; C. Doe), and rabbit anti–14-3-3 (1:200; 51-0700; Invitrogen). The carcasses were washed twice with 1× wash buffer A for 5 min each and incubated with PLA probes anti-Mouse Plus (1:5; DUO92001; Sigma-Aldrich) and anti-rabbit MINUS (1:5; DUO92005; Sigma-Aldrich) diluted in the Duolink Antibody Diluent for 1 h at 37°C. The carcasses were then washed twice with 1× wash buffer A for 5 min each and incubated in ligation solution for 30 min at 37°C. After washing twice with 1× wash buffer A for 2 min each, the carcasses were incubated in amplification solution for 100 min at 37°C. The carcasses were washed twice with 1× wash buffer B for 10 min each and washed with 0.01× wash buffer B for 1 min. The stained samples were incubated with Duolink In Situ Mounting Medium with DAPI overnight at 4°C and stored until mounting wing discs on the slides. Confocal images were collected with a 63× glycerol objective lens on the SP5 AOBS confocal microscope system.

For quantification of PLA signals, the number of PLA spots was divided by an area (30-µm square) in the mitotic zone of the wing disc proper. The "analyze particles" function of Fiji was used to automatically count PLA spot numbers (size of the particle: 0.10 to infinity).

Original data

Original data underlying this manuscript can be accessed from the Stowers Original Data Repository at https://www.stowers.org/research/publications/libpb-1419.

Online supplemental material

Fig. S1 (related to Fig. 1) shows xy and z rotation dynamics of mitotic spindle movements for control as well as z rotation dynamics for *mud-RNAi*, *scrib-RNAi*, and *dlg-RNAi*. Fig. S2 shows quantification of apico-basal polarity and junctional protein localization in wing discs expressing *scrib-RNAi* or *dlg-RNAi*. Fig. S3 (related to Fig. 3) shows spindle orientation in controls and validation of *Gli-RNAi*. Fig. S4 shows original Western blots in Fig. 4 A and also shows results of PLA (Scrib/Dlg, Scrib/Mud, and 14-3-3/Mud). Fig. S5 (related to Fig. 4) shows subcellular localization of 14-3-3 proteins in the wing disc. Table S1 (related to Fig. 4) lists the proteins copurified with Dlg or Scrib, immunoprecipitated from fly embryos, and analyzed by MudPIT mass spectrometry. Videos 1–5 show mitotic spindle movements of dividing control (Type 1: Video 1, related to Fig. 1 A; Type 2: Video 2, related to Fig. 1 B), *mud-RNAi* (Video 3, related to Fig. 1 F), *scrib-RNAi* (Video 4, related to Fig. 1 H), or *dlg-RNAi* (Video 5, related to Fig. S1 G) cells expressing Cnn-GFP and His2Av-mRFP. Video 6 (related to

Fig. S5 F) shows localization of 14-3-3ε-GFP in dividing wing disc cells.

References

Anderson, D.P., D.S. Whitney, V. Hanson-Smith, A. Woznica, W. Campodonico-Burnett, B.F. Volkman, N. King, J.W. Thornton, and K.E. Prehoda. 2016. Evolution of an ancient protein function involved in organized multicellularity in animals. *eLife.* 5:e10147. https://doi.org/10.7554/eLife.10147

Beaven, R., R.N. Bastos, C. Spanos, P. Romé, C.F. Cullen, J. Rappsilber, R. Giet, G. Goshima, and H. Ohkura. 2017. 14-3-3 regulation of Ncd reveals a new mechanism for targeting proteins to the spindle in oocytes. J. Cell Biol. 216:3029–3039. https://doi.org/10.1083/jcb.201704120

Bell, G.P., G.C. Fletcher, R. Brain, and B.J. Thompson. 2015. Aurora kinases phosphorylate Lgl to induce mitotic spindle orientation in Drosophila epithelia. Curr. Biol. 25:61–68. https://doi.org/10.1016/j.cub.2014.10.052

Bellaïche, Y., A. Radovic, D.F. Woods, C.D. Hough, M.L. Parmentier, C.J. O'Kane, P.J. Bryant, and F. Schweisguth. 2001. The Partner of Inscuteable/Discs-large complex is required to establish planar polarity during asymmetric cell division in Drosophila. Cell. 106:355–366. https://doi.org/10.1016/S0092-8674(01)00444-5

Bergstralh, D.T., H.E. Lovegrove, and D. St Johnston. 2013. Discs large links spindle orientation to apical-basal polarity in Drosophila epithelia. Curr. Biol. 23:1707–1712. https://doi.org/10.1016/j.cub.2013.07.017

Bergstralh, D.T., H.E. Lovegrove, I. Kujawiak, N.S. Dawney, J. Zhu, S. Cooper, R. Zhang, and D. St Johnston. 2016. Pins is not required for spindle orientation in the Drosophila wing disc. Development. 143:2573–2581. https://doi.org/10.1242/dev.135475

Bilder, D., and N. Perrimon. 2000. Localization of apical epithelial determinants by the basolateral PDZ protein Scribble. Nature. 403:676–680. https://doi.org/10.1038/35001108

Bilder, D., M. Li, and N. Perrimon. 2000. Cooperative regulation of cell polarity and growth by Drosophila tumor suppressors. Science. 289: 113–116. https://doi.org/10.1126/science.289.5476.113

Bosveld, F., O. Markova, B. Guirao, C. Martin, Z. Wang, A. Pierre, M. Balakireva, I. Gaugue, A. Ainslie, N. Christophorou, et al. 2016. Epithelial tricellular junctions act as interphase cell shape sensors to orient mitosis. Nature. 530:495–498. https://doi.org/10.1038/nature16970

Broadie, K., E. Rushton, E.M. Skoulakis, and R.L. Davis. 1997. Leonardo, a Drosophila 14-3-3 protein involved in learning, regulates presynaptic function. Neuron. 19:391–402. https://doi.org/10.1016/S0896-6273(00)80948-4

Buszczak, M., S. Paterno, D. Lighthouse, J. Bachman, J. Planck, S. Owen, A.D. Skora, T.G. Nystul, B. Ohlstein, A. Allen, et al. 2007. The carnegie protein trap library: a versatile tool for Drosophila developmental studies. Genetics. 175:1505–1531. https://doi.org/10.1534/genetics.106.065961

Carvalho, C.A., S. Moreira, G. Ventura, C.E. Sunkel, and E. Morais-de-Sá. 2015. Aurora A triggers Lgl cortical release during symmetric division to control planar spindle orientation. Curr. Biol. 25:53–60. https://doi.org/10.1016/j.cub.2014.10.053

Chang, H.C., and G.M. Rubin. 1997. 14-3-3 epsilon positively regulates Ras-mediated signaling in Drosophila. Genes Dev. 11:1132–1139. https://doi.org/10.1101/gad.11.9.1132

De, S., and D. Kline. 2013. Evidence for the requirement of 14-3-3eta (YWHAH) in meiotic spindle assembly during mouse oocyte maturation. BMC Dev. Biol. 13:10. https://doi.org/10.1186/1471-213X-13-10

Dewey, E.B., D. Sanchez, and C.A. Johnston. 2015. Warts phosphorylates mud to promote pins-mediated mitotic spindle orientation in Drosophila, independent of Yorkie. Curr. Biol. 25:2751–2762. https://doi.org/10.1016/j.cub.2015.09.025

di Pietro, F., A. Echard, and X. Morin. 2016. Regulation of mitotic spindle orientation: an integrated view. EMBO Rep. 17:1106–1130. https://doi.org/10.15252/embr.201642292

Durgan, J., N. Kaji, D. Jin, and A. Hall. 2011. Par6B and atypical PKC regulate mitotic spindle orientation during epithelial morphogenesis. J. Biol. Chem. 286:12461–12474. https://doi.org/10.1074/jbc.M110.174235

Eng, J.K., A.L. McCormack, and J.R. Yates III. 1994. An approach to correlate tandem mass spectral data of peptides with amino acid sequences in a protein database. J. Am. Soc. Mass Spectrom. 5:976–989. https://doi.org/10.1016/1044-0305(94)80016-2

Florens, L., and M.P. Washburn. 2006. Proteomic analysis by multidimensional protein identification technology. Methods Mol. Biol. 328:159–175.

Freeman, A.K., and D.K. Morrison. 2011. 14-3-3 Proteins: diverse functions in cell proliferation and cancer progression. Semin. Cell Dev. Biol. 22: 681–687. https://doi.org/10.1016/j.semcdb.2011.08.009

Gardino, A.K., and M.B. Yaffe. 2011. 14-3-3 proteins as signaling integration points for cell cycle control and apoptosis. Semin. Cell Dev. Biol. 22: 688–695. https://doi.org/10.1016/j.semcdb.2011.09.008

Gillies, T.E., and C. Cabernard. 2011. Cell division orientation in animals. Curr. Biol. 21:R599–R609. https://doi.org/10.1016/j.cub.2011.06.055

Gloerich, M., J.M. Bianchini, K.A. Siemers, D.J. Cohen, and W.J. Nelson. 2017. Cell division orientation is coupled to cell-cell adhesion by the E-cadherin/LGN complex. Nat. Commun. 8:13996. https://doi.org/10.1038/ncomms13996

Guilgur, L.G., P. Prudêncio, T. Ferreira, A.R. Pimenta-Marques, and R.G. Martinho. 2012. Drosophila aPKC is required for mitotic spindle orientation during symmetric division of epithelial cells. Development. 139: 503–513. https://doi.org/10.1242/dev.071027

Hao, Y., Q. Du, X. Chen, Z. Zheng, J.L. Balsbaugh, S. Maitra, J. Shabanowitz, D.F. Hunt, and I.G. Macara. 2010. Par3 controls epithelial spindle orientation by aPKC-mediated phosphorylation of apical Pins. Curr. Biol. 20:1809–1818. https://doi.org/10.1016/j.cub.2010.09.032

Jaffe, A.B., N. Kaji, J. Durgan, and A. Hall. 2008. Cdc42 controls spindle orientation to position the apical surface during epithelial morphogenesis. J. Cell Biol. 183:625–633. https://doi.org/10.1083/jcb.200807121

Johnston, C.A., K. Hirono, K.E. Prehoda, and C.Q. Doe. 2009. Identification of an Aurora-A/PinsLINKER/Dlg spindle orientation pathway using induced cell polarity in S2 cells. Cell. 138:1150–1163. https://doi.org/10.1016/j.cell.2009.07.041

Keder, A., N. Rives-Quinto, B.L. Aerne, M. Franco, N. Tapon, and A. Carmena. 2015. The hippo pathway core cassette regulates asymmetric cell division. Curr. Biol. 25:2739–2750. https://doi.org/10.1016/j.cub.2015.08.064

Konno, D., G. Shioi, A. Shitamukai, A. Mori, H. Kiyonari, T. Miyata, and F. Matsuzaki. 2008. Neuroepithelial progenitors undergo LGN-dependent planar divisions to maintain self-renewability during mammalian neurogenesis. Nat. Cell Biol. 10:93–101. https://doi.org/10.1038/ncb1673

Le, T.P., L.T. Vuong, A.R. Kim, Y.C. Hsu, and K.W. Choi. 2016. 14-3-3 proteins regulate Tctp-Rheb interaction for organ growth in Drosophila. Nat. Commun. 7:11501. https://doi.org/10.1038/ncomms11501

Lee, T., and L. Luo. 1999. Mosaic analysis with a repressible cell marker for studies of gene function in neuronal morphogenesis. Neuron. 22: 451–461. https://doi.org/10.1016/S0896-6273(00)80701-1

Lu, M.S., and C.A. Johnston. 2013. Molecular pathways regulating mitotic spindle orientation in animal cells. Development. 140:1843–1856. https://doi.org/10.1242/dev.087627

Lu, M.S., and K.E. Prehoda. 2013. A NudE/14-3-3 pathway coordinates dynein and the kinesin Khc73 to position the mitotic spindle. Dev. Cell. 26: 369–380. https://doi.org/10.1016/j.devcel.2013.07.021

Macara, I.G., R. Guyer, G. Richardson, Y. Huo, and S.M. Ahmed. 2014. Epithelial homeostasis. Curr. Biol. 24:R815–R825. https://doi.org/10.1016/j.cub.2014.06.068

Mahale, S., M. Kumar, A. Sharma, A. Babu, S. Ranjan, C. Sachidanandan, and S.V.S. Mylavarapu. 2016. The Light Intermediate Chain 2 Subpopulation of Dynein Regulates Mitotic Spindle Orientation. Sci. Rep. 6:22. https://doi.org/10.1038/s41598-016-0030-3

Megraw, T.L., S. Kilaru, F.R. Turner, and T.C. Kaufman. 2002. The centrosome is a dynamic structure that ejects PCM flares. J. Cell Sci. 115: 4707–4718. https://doi.org/10.1242/jcs.00134

Meyer, E.J., A. Ikmi, and M.C. Gibson. 2011. Interkinetic nuclear migration is a broadly conserved feature of cell division in pseudostratified epithelia. Curr. Biol. 21:485–491. https://doi.org/10.1016/j.cub.2011.02.002

Morin, X., and Y. Bellaïche. 2011. Mitotic spindle orientation in asymmetric and symmetric cell divisions during animal development. Dev. Cell. 21: 102–119. https://doi.org/10.1016/j.devcel.2011.06.012

Morin, X., R. Daneman, M. Zavortink, and W. Chia. 2001. A protein trap strategy to detect GFP-tagged proteins expressed from their endogenous loci in Drosophila. Proc. Natl. Acad. Sci. USA. 98:15050–15055. https://doi.org/10.1073/pnas.261408198

Morin, X., F. Jaouen, and P. Durbec. 2007. Control of planar divisions by the G-protein regulator LGN maintains progenitors in the chick neuroepithelium. Nat. Neurosci. 10:1440–1448. https://doi.org/10.1038/nn1984

Muzzopappa, M., L. Murcia, and M. Milán. 2017. Feedback amplification loop drives malignant growth in epithelial tissues. Proc. Natl. Acad. Sci. USA. 114:E7291–E7300. https://doi.org/10.1073/pnas.1701791114

Nakajima, Y.I. 2018. Mitotic spindle orientation in epithelial homeostasis and plasticity. J. Biochem. 164:277–284. https://doi.org/10.1093/jb/mvy064

Nakajima, Y., E.J. Meyer, A. Kroesen, S.A. McKinney, and M.C. Gibson. 2013. Epithelial junctions maintain tissue architecture by directing planar spindle orientation. Nature. 500:359–362. https://doi.org/10.1038/nature12335

Noatynska, A., M. Gotta, and P. Meraldi. 2012. Mitotic spindle (DIS)orientation and DISease: cause or consequence? J. Cell Biol. 199:1025–1035. https://doi.org/10.1083/jcb.201209015

Padash-Barmchi, M., K. Charish, J. Que, and V.J. Auld. 2013. Gliotactin and Discs large are co-regulated to maintain epithelial integrity. J. Cell Sci. 126:1134–1143. https://doi.org/10.1242/jcs.113803

Pandey, R., S. Heidmann, and C.F. Lehner. 2005. Epithelial re-organization and dynamics of progression through mitosis in Drosophila separase complex mutants. J. Cell Sci. 118:733–742. https://doi.org/10.1242/jcs.01663

Pavelka, N., M.L. Fournier, S.K. Swanson, M. Pelizzola, P. Ricciardi-Castagnoli, L. Florens, and M.P. Washburn. 2008. Statistical similarities between transcriptomics and quantitative shotgun proteomics data. Mol. Cell. Proteomics. 7:631–644. https://doi.org/10.1074/mcp.M700240-MCP200

Pease, J.C., and J.S. Tirnauer. 2011. Mitotic spindle misorientation in cancer--out of alignment and into the fire. J. Cell Sci. 124:1007–1016. https://doi.org/10.1242/jcs.081406

Peyre, E., F. Jaouen, M. Saadaoui, L. Haren, A. Merdes, P. Durbec, and X. Morin. 2011. A lateral belt of cortical LGN and NuMA guides mitotic spindle movements and planar division in neuroepithelial cells. J. Cell Biol. 193:141–154. https://doi.org/10.1083/jcb.201101039

Poulton, J.S., J.C. Cuningham, and M. Peifer. 2014. Acentrosomal Drosophila epithelial cells exhibit abnormal cell division, leading to cell death and compensatory proliferation. Dev. Cell. 30:731–745. https://doi.org/10.1016/j.devcel.2014.08.007

Qin, Y., W.H. Meisen, Y. Hao, and I.G. Macara. 2010. Tuba, a Cdc42 GEF, is required for polarized spindle orientation during epithelial cyst formation. J. Cell Biol. 189:661–669. https://doi.org/10.1083/jcb.201002097

Ragkousi, K., and M.C. Gibson. 2014. Cell division and the maintenance of epithelial order. J. Cell Biol. 207:181–188. https://doi.org/10.1083/jcb.201408044

Ragkousi, K., K. Marr, S. McKinney, L. Ellington, and M.C. Gibson. 2017. Cell-Cycle-Coupled Oscillations in Apical Polarity and Intercellular Contact Maintain Order in Embryonic Epithelia. Curr. Biol. 27:1381–1386. https://doi.org/10.1016/j.cub.2017.03.064

Ren, F., L. Zhang, and J. Jiang. 2010. Hippo signaling regulates Yorkie nuclear localization and activity through 14-3-3 dependent and independent mechanisms. Dev. Biol. 337:303–312. https://doi.org/10.1016/j.ydbio.2009.10.046

Rodriguez-Fraticelli, A.E., S. Vergarajauregui, D.J. Eastburn, A. Datta, M.A. Alonso, K. Mostov, and F. Martín-Belmonte. 2010. The Cdc42 GEF Intersectin 2 controls mitotic spindle orientation to form the lumen during epithelial morphogenesis. J. Cell Biol. 189:725–738. https://doi.org/10.1083/jcb.201002047

Saadaoui, M., M. Machicoane, F. di Pietro, F. Etoc, A. Echard, and X. Morin. 2014. Dlg1 controls planar spindle orientation in the neuroepithelium through direct interaction with LGN. J. Cell Biol. 206:707–717. https://doi.org/10.1083/jcb.201405060

Schulte, J., K. Charish, J. Que, S. Ravn, C. MacKinnon, and V.J. Auld. 2006. Gliotactin and Discs large form a protein complex at the tricellular junction of polarized epithelial cells in Drosophila. J. Cell Sci. 119: 4391–4401. https://doi.org/10.1242/jcs.03208

Siegrist, S.E., and C.Q. Doe. 2005. Microtubule-induced Pins/Galphai cortical polarity in Drosophila neuroblasts. Cell. 123:1323–1335. https://doi.org/10.1016/j.cell.2005.09.043

Söderberg, O., M. Gullberg, M. Jarvius, K. Ridderstråle, K.J. Leuchowius, J. Jarvius, K. Wester, P. Hydbring, F. Bahram, L.G. Larsson, and U. Landegren. 2006. Direct observation of individual endogenous protein complexes in situ by proximity ligation. Nat. Methods. 3:995–1000. https://doi.org/10.1038/nmeth947

Su, T.T., D.H. Parry, B. Donahoe, C.T. Chien, P.H. O'Farrell, and A. Purdy. 2001. Cell cycle roles for two 14-3-3 proteins during Drosophila development. J. Cell Sci. 114:3445–3454.

Tabb, D.L., W.H. McDonald, and J.R. Yates III. 2002. DTASelect and Contrast: tools for assembling and comparing protein identifications from shotgun proteomics. J. Proteome Res. 1:21–26. https://doi.org/10.1021/pr015504q

Tuncay, H., B.F. Brinkmann, T. Steinbacher, A. Schürmann, V. Gerke, S. Iden, and K. Ebnet. 2015. JAM-A regulates cortical dynein localization through Cdc42 to control planar spindle orientation during mitosis. Nat. Commun. 6:8128. https://doi.org/10.1038/ncomms9128

Udan, R.S., M. Kango-Singh, R. Nolo, C. Tao, and G. Halder. 2003. Hippo promotes proliferation arrest and apoptosis in the Salvador/Warts pathway. Nat. Cell Biol. 5:914–920. https://doi.org/10.1038/ncb1050

Vizcaíno, J.A., E.W. Deutsch, R. Wang, A. Csordas, F. Reisinger, D. Ríos, J.A. Dianes, Z. Sun, T. Farrah, N. Bandeira, et al. 2014. ProteomeXchange provides globally coordinated proteomics data submission and dissemination. Nat. Biotechnol. 32:223–226. https://doi.org/10.1038/nbt.2839

Woods, D.F., and P.J. Bryant. 1989. Molecular cloning of the lethal(1)discs large-1 oncogene of Drosophila. Dev. Biol. 134:222–235. https://doi.org/10.1016/0012-1606(89)90092-4

Xu, T., W. Wang, S. Zhang, R.A. Stewart, and W. Yu. 1995. Identifying tumor suppressors in genetic mosaics: the Drosophila lats gene encodes a putative protein kinase. Development. 121:1053–1063.

Yu, F., X. Morin, Y. Cai, X. Yang, and W. Chia. 2000. Analysis of partner of inscuteable, a novel player of Drosophila asymmetric divisions, reveals two distinct steps in inscuteable apical localization. Cell. 100:399–409. https://doi.org/10.1016/S0092-8674(00)80676-5

Yu, F., Y. Cai, R. Kaushik, X. Yang, and W. Chia. 2003. Distinct roles of Galphai and Gbeta13F subunits of the heterotrimeric G protein complex in the mediation of Drosophila neuroblast asymmetric divisions. J. Cell Biol. 162:623–633. https://doi.org/10.1083/jcb.200303174

Zeitler, J., C.P. Hsu, H. Dionne, and D. Bilder. 2004. Domains controlling cell polarity and proliferation in the Drosophila tumor suppressor Scribble. J. Cell Biol. 167:1137–1146. https://doi.org/10.1083/jcb.200407158

Zhang, Y., Z. Wen, M.P. Washburn, and L. Florens. 2010. Refinements to label free proteome quantitation: how to deal with peptides shared by multiple proteins. Anal. Chem. 82:2272–2281. https://doi.org/10.1021/ac9023999

Zheng, Z., H. Zhu, Q. Wan, J. Liu, Z. Xiao, D.P. Siderovski, and Q. Du. 2010. LGN regulates mitotic spindle orientation during epithelial morphogenesis. J. Cell Biol. 189:275–288. https://doi.org/10.1083/jcb.200910021

Zhou, Q., Y.S. Kee, C.C. Poirier, C. Jelinek, J. Osborne, S. Divi, A. Surcel, M.E. Will, U.S. Eggert, A. Müller-Taubenberger, et al. 2010. 14-3-3 coordinates microtubules, Rac, and myosin II to control cell mechanics and cytokinesis. Curr. Biol. 20:1881–1889. https://doi.org/10.1016/j.cub.2010.09.048